Near-field radiative thermal transfer between a nanostructured periodic material and a planar substrate

Hamidreza Chalabi, Erez Hasman, and Mark L. Brongersma

Phys. Rev. B **91**, 014302 — Published 6 January 2015

DOI: 10.1103/PhysRevB.91.014302

Near-field radiative thermal transfer between a nano-structured periodic material and a planar substrate

Hamidreza Chalabi,[1,*] Erez Hasman,[2,†] and Mark L. Brongersma[1,‡]

[1] *Geballe Laboratory for Advanced Materials, Stanford University, Stanford, California 94305, USA*
[2] *Micro and Nanooptics Laboratory, Faculty of Mechanical Engineering, and Russel Berrie Nanotechnology Institute, Technion-Israel Institute of Technology, Haifa 32000, Israel*

This paper provides a method based on rigorous coupled wave analysis for the calculation of the radiative thermal conductance between a layer that is patterned with arbitrary, periodically repeating features and a planar substrate. This method is applied to study the transfer from an array of beams with a rectangular cross section. The impact of the structure size and spacing on the thermal conductance are investigated. These calculations are compared to an effective medium theory, which becomes increasingly accurate as the structure sizes fall well below the relevant resonance wavelengths of materials and structures. Moreover, comparisons are made with a modified proximity approximation and the far-field approximation, which become valid for small and large spacings, respectively. Results show that new levels of control over the magnitude and spectral contributions to thermal conductance can be achieved with corrugated structures relative to planar ones. Specifically, we show for SiC arrays with rectangular cross sections and with the same filling fraction that the use of a smaller periodicity leads to a lowered far-field thermal transfer and an increased near-field thermal transfer.

INTRODUCTION:

The control of thermal emission is critical to a variety of applications such as energy conversion[1,2], imaging[3] and thermal emitters[4,5]. One way to achieve control over thermal emission is by manipulating the near-field surrounding optically-resonant nanostructures[6,7]. Radiative thermal transfer between two objects which obeys Planck's law[8] in the far-field limit shows a dramatic enhancement when the separation is reduced to such an extent that near-field effects dominate the thermal transfer[9–11]. Near-field effects cause a redistribution of the local density of states (LDOS) and enable evanescent waves to make the most significant contribution to the total thermal transfer. In addition to the total magnitude of the thermal transfer, the spectral contributions also dramatically change in the near-field regime[10].

Recent developments in area of nanophotonics have inspired efforts to use structures with subwavelength features for the purpose of controlling radiative thermal transfer. An exact theory is available to quantify the thermal transfer between an arbitrary number of arbitrarily shaped objects[12]. However, finding numerical solutions for seemingly simple geometries (e.g. a nanoparticle above a plane) requires tremendous computational power as multiple frequencies and length scales are involved. For this reason, there have been intense efforts to develop new, efficient numerical techniques that enable calculation of thermal transfer in specific geometries. This enabled calculation of thermal transfer in important basic geometries, such as planar-to-planar[9,13,14] as well as planar structures to a sphere[15–17], a cylinder[17], and even a cone[17]. A good review that summarizes the results of such studies is given in reference[18].

In addition to the development of faster numerical techniques, physical insight is also used to improve the speed by making certain reasonable approximations. For example, effective medium theory has been used to speed up calculation of the thermal transfer between subwavelength periodic structures[19–23]. This theory transforms high spatial frequency structures to uniform, simple structures for which the variations in optical properties occur just along a single dimension creating a stratified medium; after that, theories to deal with stratified media[9] can be applied for calculation of the thermal transfer. Effective medium theories cannot handle periodic structures with structure sizes that are not deep-subwavelength for all of the relevant wavelengths in the problem. Here, the relevant wavelengths can be linked to materials-related resonances (e.g. plasmonic or phononic) or structure related resonances (e.g. Mie or grating resonances).

In this paper we theoretically derive an expression for the radiative thermal heat transfer in periodic structures based on rigorous coupled wave analysis (RCWA) method that can handle such structures. This enables one to access new physical regimes and to discover and systematically analyze new physical phenomena in thermal transfer physics. Thermal emission from periodic structures to air is investigated in several references[24,25]. Moreover, the thermal transfer between two gratings with semi-infinite sizes is investigated using the scattering method, recently[26,27]. The scattering trace formulas have also been incorporated for structures made of multiple bodies[28]. Here, we consider the thermal transfer between a finite-sized nano-structured periodic material and a planar structure in the near-field regime. The RCWA technique together with the possible use of symmetries in a system boosts the numerical efficiency compared with the simulations that has been done for calculation of thermal transfer between grating structures using the Finite-difference time-domain (FDTD) method, recently[29]. Moreover, for comparison purposes, some approximation methods are developed for thermal transfer

calculation. One well known method for near-field thermal transfer calculation is the proximity method[30–32]. Here, since the periodic structure can have a finite-sized height, the proximity method is generalized to take care of such finiteness. On the other hand in the far-field regime, the thermal transfer can be calculated based on knowledge of the directional emissivity of the substrate.

The RCWA formalism provides significant flexibility to include arbitrarily shaped nanostructures and good criteria for determining the accuracy of obtained results based on convergence by increasing the number of spatial harmonics. Our proposed method bears some resemblance to the scattering method[15,33] in its final form; however, there are some distinguishing technical differences. Our method also provides a very direct way for determining the variation in thermal transfer across a period in the periodic structures. This variation can itself give important information to determine whether the periodicity is in the subwavelength regime or not. For instance, in the regime that periodicity is on the same order or even larger than the pertinent resonance wavelength, one would intuitively expect that the thermal transfer flow to be maximized in the regions where the top and bottom layer are closer together and vice versa. In fact, in this regime the total thermal transfer can be seen as a superposition of parallel channels corresponding to regions with different gap sizes, in which the contribution of each channel is dependent on the local gap size. This decomposition breaks down in the regime that periodicity becomes subwavelength, in which effective medium theory becomes more accurate, and the interference between two adjacent regions becomes increasingly important. In the deep subwavelength regime, thermal transfer should have negligible variation across the period.

It should be noted that there are some recent proposed techniques such as using of trace formulas based on the boundary element methods[34] for thermal transfer calculation. In addition, there are some available Eigen-mode expansion methods[35] for this purpose. However, the superiority of the proposed method is that it does not need to find a proper orthonormal basis based on the geometry of the structure. Furthermore, it does not require carrying out FDTD simulations for obtaining the spectral energy flux from each mode.

Use of the RCWA method for obtaining electromagnetic field patterns is quite common in nanophotonics. A numerically stable version of this method was first developed by moharam[36,37], and this technique can be used to obtain electromagnetic field distributions developed around arbitrary periodic structures under plane wave incident field illumination. However, for thermal transfer calculations we will use it to calculate the Green's functions that capture the electromagnetic field responses to arbitrarily located and oriented electric dipoles. For calculation of the Green's functions with the RCWA method we have made use of the modified Sipe's formalism[25,38].

In continuation, the derived method is used for calculation of the thermal conductance between a SiC slab and an array of SiC beams of rectangular cross section. Here, the dependence of the thermal transfer on beam size is explored. Silicon carbide is a polar semiconductor and its surface supports electromagnetic waves coupled to collective lattice vibrations known as surface phonon polaritons (SPhPs). These surface waves which are in the infrared spectral region provide the main channels for thermal transfer in the near-field regime for such materials. The numerical calculations are done for spacings and periodicities that span several orders of magnitudes to explore different physical regimes for the thermal transport. Since SiC has a phononic resonance wavelength around 10μm, we also expect Mie resonances to show up themselves in these range of distances. Our calculations verify this hypothesis by showing that in this range of distances, the thermal conductance obtains its maximum value for non planar structures. This observation demonstrates that periodic structures can be used to reach new levels of control over thermal transfer and afford access to new resonant pathways that enhance or spectrally control the thermal transfer.

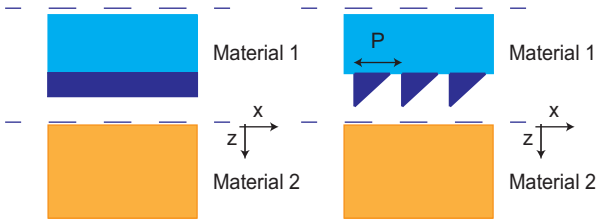

Figure 1: Schematic of (a) planar structured materials and (b) a planar and an arbitrary shaped periodic structure that will be analyzed in thermal transfer calculations.

EXACT THEORY:

Before deriving the theory used for calculating the thermal transfer from a periodic to a planar structure, it is educational to briefly review the derivation of Green's functions in planar structures through the use of Sipe's method[38]. Thermal transfer calculations involving planar structures were first done by Van hove and Polder in 1971[9]. Sipe showed how the required Green's functions for calculation of thermal transfer can be re-derived in a convenient form for an arbitrary stack of planar materials. The first section of the supplemental material[39] is devoted to this re-derivation. This corresponds to calculation of Green's functions in structures like the one shown in Fig. 1a. Generalizing Sipe's approach, Green's functions can be obtained for periodic structures. Those Green's functions can be used later for obtaining the thermal transfer through calculation of the Poynting vector that captures the thermal power flow from one medium

to another. A schematic of the type of periodic structures of interest is illustrated in Fig. 1b. For illustration purposes and to simplify the math involved, we restrict ourselves to have one of the materials to be planar (shown as material 2).

For calculation of the near-field thermal transfer, the Green's functions $\overrightarrow{G_E^a}(\omega, x, y, z, k_x, k_y)$ and $\overrightarrow{G_H^a}(\omega, x, y, z, k_x, k_y)$ are defined as follows:

$$\overrightarrow{G_E^a}(\omega, x, y, z, k_x, k_y) \triangleq \frac{-\omega\mu_0}{2k_z} \times \sum_b \left(\overrightarrow{Res_E}\left(\omega, x, y, z, \beta\hat{\beta}, z'=0, \hat{p}_{2+}\right)\hat{p}_{2+} + \overrightarrow{Res_E}\left(\omega, x, y, z, \beta\hat{\beta}, z'=0, \hat{s}\right)\hat{s}\right)_{ba}\hat{e}_b \quad (1)$$

$$\overrightarrow{G_H^a}(\omega, x, y, z, k_x, k_y) \triangleq \frac{-\omega\mu_0}{2k_z} \times \sum_b \left(\overrightarrow{Res_H}\left(\omega, x, y, z, \beta\hat{\beta}, z'=0, \hat{p}_{2+}\right)\hat{p}_{2+} + \overrightarrow{Res_H}\left(\omega, x, y, z, \beta\hat{\beta}, z'=0, \hat{s}\right)\hat{s}\right)_{ba}\hat{e}_b \quad (2)$$

where $\hat{e}_b$ is the unity vector in direction b, which takes on the unity vectors in x, y, and z directions in the summation. These are the electric and magnetic fields at position x, y, and z, produced by the unity component a of the current density at $z'=0$, respectively. Note that $\overrightarrow{Res_E}\left(\omega, x, y, z, \beta\hat{\beta}, z'=0, \hat{p}_{2+}\right)$, $\overrightarrow{Res_E}\left(\omega, x, y, z, \beta\hat{\beta}, z'=0, \hat{s}\right)$ are the electric field responses at position x, y, and z to P and S polarized incident plane waves with transversal wave vector $\beta\hat{\beta}$ and unity electric field amplitude at position $z'=0$ and angular frequency of ω. Similarly, $\overrightarrow{Res_H}\left(\omega, x, y, z, \beta\hat{\beta}, z'=0, \hat{p}_{2+}\right)$, and $\overrightarrow{Res_H}\left(\omega, x, y, z, \beta\hat{\beta}, z'=0, \hat{s}\right)$ are the corresponding magnetic field responses. These vector quantities can be obtained through the RCWA method. The above equations are modified versions of Sipe's formalism[38] as applied to periodic structures.

Moreover, we know that fluctuating current densities inside a material that is in thermodynamic equilibrium at a temperature T, obey the following correlation relation known as the fluctuation dissipation theorem[40,41]:

$$\left\langle \vec{J}_a(\omega, \vec{r_0})\, \vec{J}_b^*\left(\omega', \vec{r_0'}\right)\right\rangle = 4\pi\epsilon_0\epsilon''(\omega)\hbar\omega^2 \times \left(e^{\hbar\omega/k_bT}-1\right)^{-1}\delta_{ab}\delta(\omega-\omega')\,\delta\left(\vec{r_0}-\vec{r_0'}\right) \quad (3)$$

Using the above equations and after a somewhat tedious derivation[39], the following expression is obtained for the thermal conduction:

$$S_{total}(x) = \frac{1}{4\pi^3}\sum_a \int_{\omega=0}^{+\infty} d\omega\epsilon_0\epsilon''(\omega)\left(e^{\hbar\omega/k_bT}-1\right)^{-2} \times \int_{k_y=-\infty}^{+\infty}\int_{k_x=-\infty}^{+\infty} dk_x dk_y \frac{e^{\hbar\omega/k_bT}}{Im(k_z)}\frac{\hbar^2\omega^3}{k_bT^2} \times \Re\Big\{\Big(\overrightarrow{G_E^a}(\omega, x, y=0, z=0, k_x, k_y) \times \overrightarrow{G_H^{a*}}(\omega, x, y=0, z=0, k_x, k_y) - \overrightarrow{G_E^a}(\omega, x, y=0, z=-h, k_x, k_y) \times \overrightarrow{G_H^{a*}}(\omega, x, y=0, z=-h, k_x, k_y)\Big)_z\Big\} \quad (4)$$

In fact, what is measured as the total heat conductance is the average of the above function across a period, which we show here with the same symbol:

$$S_{total} = \frac{1}{P}\int_{x=0}^{P} S_{total}(x)\,dx \quad (5)$$

We have assumed that the periodic material is located between planes $z=0$ and $z=-h$. In the case that the periodically structured material extends to infinity, we should simply neglect the terms corresponding to $z=-h$ in the Eq. 4.

It is important to note that considering only the fields in a line in the x-direction saves significant computational time. In fact this is achieved by exploiting the translational symmetry of our structure in y-direction and also the fact that for obtaining the energy flow, it is sufficient to calculate the Poynting vector in a cross section. Note that in our method, the variation in the thermal transfer across a period can also be obtained. This provides the ability to determine the contributions of different locations across the period to the total thermal transfer or conductance.

Moreover, in the above calculations, we are involved with only transverse components of the electromagnetic fields. Since these quantities are continuous across the barrier, we need only to calculate the electromagnetic fields in the substrate right at the boundary and also in the plane $z=-h$ right outside the periodic material. Electromagnetic fields in the substrate right at the boundary can be calculated from the reflection coefficients in the RCWA formalism. Similarly, electromagnetic fields right outside the periodic material can be calculated from transmission coefficients. This will further simplify the required RCWA calculations since the calculation of the electromagnetic fields in the middle layers are not needed anymore. [See section 7 of reference[37]]

APPROXIMATION METHODS:

Far-Field Approximation Method:

For calculation of the thermal transfer in the far-field regime, we can use the fact that the directional emissivity of the substrate is given by the $e_p(\theta) = 1 - |R_p(\theta)|^2$ and $e_s(\theta) = 1 - |R_s(\theta)|^2$ corresponding to the p and s polarizations, respectively[42]. Then the thermal transfer can be calculated based on how much the emitted power is absorbed by the periodic structure. To first order, if we neglect the contribution of the rays after reflection from the top structure and returning to it after reflection from substrate, we have:

$$S(\omega) = \frac{\hbar^2\omega^4}{8\pi^3 c^2 k_b T^2}\left(e^{\frac{\hbar\omega}{k_b T}} - 1\right)^{-2} e^{\frac{\hbar\omega}{k_b T}} \times \int_0^{2\pi}\int_0^{\frac{\pi}{2}} sin(\theta)\, cos(\theta)\, d\theta d\phi \times \left(e_p(\theta) A_p(\theta,\phi) + e_s(\theta) A_s(\theta,\phi)\right) \quad (6)$$

where in that $A_p(\theta,\phi)$ and $A_s(\theta,\phi)$ corresponds to the absorption of the periodic structure at an azimuthal angle ϕ and a polar angle θ for p and s polarizations, respectively.

Since the contributions of the rays undergoing two or more reflections to the thermal transfer are neglected, this approximation gives a lower limit to the exact thermal transfer in the far-field regime.

Modified Proximity Method:

For calculations in the near-field regime, the proximity method is perhaps the most popular one[30–32]. However, in its original form the two bodies are assumed to have semi-infinite height. Here, since the periodic structure can have a finite height, the proximity method has to be generalized. In this method, thermal transfer is calculated across a period, based on the distance of the two bodies and the height of the periodic structure at that point. According to this method, for an array of beams with rectangular cross section, thermal transfer should vary in proportion to the filling fraction (FF), which is defined as the ratio of the beam width to the periodicity.

NUMERICAL SIMULATIONS:

In the following, we consider a periodic array of SiC beams of rectangular cross section placed above a continuous slab of SiC (Fig. 2). Using our developed formalism, the thermal conductance between the SiC beams and the slab of SiC is numerically calculated. The details of the notations used for the parameters involved in this structure are shown in Fig. 2. Calculations for this structure

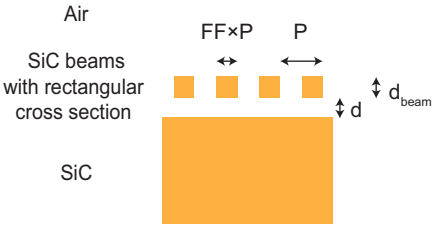

Figure 2: SiC beams with a rectangular cross section are placed in front of a SiC substrate. The width of each beam is assumed to be $FF \times P$, and they are separated by a distance P from each other. The distances involved for this structure are shown in the figure.

have been done for four different separations between the two SiC structures (specifically $d = 50\mu m$, $d = 5\mu m$, $d = 0.5\mu m$, and $d = 0.05\mu m$) and different periodicities (specifically $P = 1um$, $P = 10um$, and $P = 0.1um$). The height of the beams in the considered structures is $d_{beam} = 5\mu m$.

Based on references[43,44], it is assumed that the relative permittivity of SiC can be written as $\epsilon = \epsilon_\infty + \omega_0^2(\epsilon_s - \epsilon_\infty)\left(\omega_0^2 - \omega^2 + i\omega\delta\right)^{-1}$, with $\epsilon_\infty = 6.7$, $\epsilon_s = 10$, $\delta/\omega_0 = 0.006$ and $\omega_0/(2\pi) = 2.38 \times 10^{13} sec^{-1}(12.6\mu m)$. The frequency variations of the real and imaginary parts of this relative permittivity are plotted in Fig. 3. In addition, the temperature that is assumed in the numerical calculations is $T = 315K$.

Numerical Implementation:

For calculations based on the RCWA method, it is well-known that increasing the number of harmonics leads to a more accurate determination of the field distributions. However, this increase will lead to an increase in computational time as well. Since the numerical evaluation of the thermal conductance by the presented method involves inverting $4n \times 4n$ matrices, the computational time grows with the cube of the number of harmonics incorporated. It is clear from the last equation in theory section that obtaining the spectral thermal conductance at a specific frequency requires two dimensional integrations in the k_x, k_y plane. For each value of k_x and k_y, a RCWA calculation should be carried out to obtain the corresponding integrand. This clarifies the importance of identifying a fast integration technique to maximize the speed of calculations. We have used the VEGAS method for integration in k_x, k_y plane which is based on Monte Carlo important sampling of the integrand function[45]. To verify our calculation technique, we first accurately reproduced the results for the limiting cases of gratings with filling fractions of 0 and 1. In those cases, using just one harmonic will lead to the precise result and the RCWA method will converge to the results that can be obtained with the transfer matrix method for a stratified medium consisting of uniform layers. In these extreme

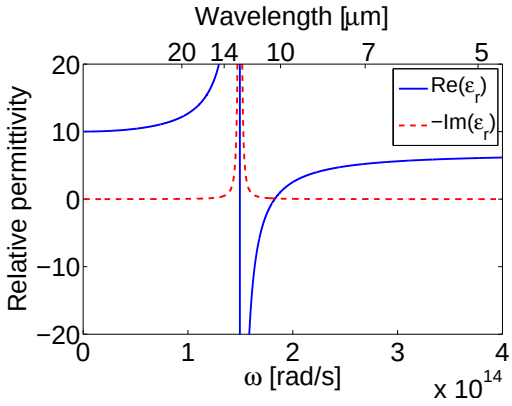

Figure 3: Frequency variations of the real and imaginary parts of SiC relative permittivity.

cases we can simply use the planar methods developed by Polder and Van hove[9].

For this study, these numerical calculations were run on a node with 16 CPUs using MPI[46] for parallelization (The node that we used for our calculations has 16 processors of 2.67 GHz Intel Xeon X5550). The time required for obtaining each set of results on a single node for the case of 21 harmonics was around 10 hours. However, this can be decreased by capitalizing on certain symmetries in specific periodic structures, which has been proposed for the 2D grating in reference[47] and can be incorporated in 1D grating structures as well (using for instance the inversion symmetry present in the binary grating).

To study the convergence of the results with the number of harmonics, calculations were made with 4 different numbers of harmonics: 1, 5, 11, and 21. Obtained results show that for the considered structures, the thermal conductance converges with less than 2% error by incorporating 21 harmonics without the need for using more harmonics.

Numerical Results:

One important fact that can be derived from the obtained results is that, as the periodicity decreases, the result obtained with using just one harmonic becomes more accurate. This is to be expected since in the case of incorporating just one harmonic, our method reproduces results obtained by the effective medium theory (EMT) which becomes increasingly accurate in subwavelength regime (compared with the surface phonon polariton resonance wavelength). Note that in the case of using just one harmonic, the permittivity of each layer is replaced by a constant value across the period. This constant value, however, takes on different magnitudes depending on the incident electric field direction. This is the case also in the effective medium theories[19–23], used for calculation of the thermal transfer, in which effective

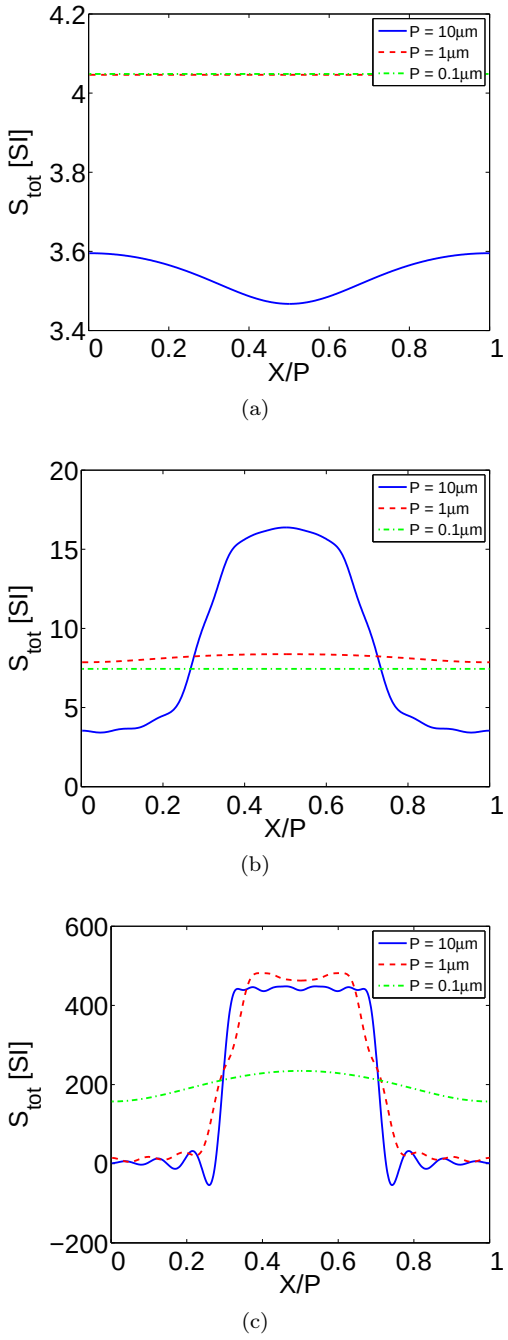

Figure 4: Contributions to the thermal conductance for the structure shown in Fig. 2 across a period for different values of periodicity, by assuming a constant value of $FF = 0.4$, in the case of (a) $d = 5\mu m$ (b) $d = 0.5\mu m$ (c) $d = 0.05\mu m$.

permittivities of different layers are calculated as constant tensorial quantities. In this regard, our proposed method can be used to determine the accuracy of the effective medium theory and how the actual responses are deviating from it.

Figure 4 shows the contribution of different points

across the period to the total thermal conductance. In this figure the thermal conductance is plotted as a function of position x across the period at the $z = 0$ plane for different values of periodicity and distances. The filling fraction is assumed to be the same value of 0.4 in all cases. Note that since we have translational symmetry in the y direction, there is no change in thermal conductance in that direction. This figure verifies the fact that the thermal conductance in the limit of small periods tends toward a constant value across the period which can be obtained by effective medium theory. On the other hand, this figure further demonstrates that for periodicities larger than some critical value, the thermal conductance can be modeled as a superposition of two channels; a channel with larger thermal conductance which is due to parts of slabs that are closer together and the other one with smaller thermal conductance which is due to the sections that are farther from each other. These plots were obtained by incorporation of 21 harmonics. Note that these plots show the total thermal conductance from the substrate to outside and do consider the part of it that goes outside the array of beams, as well.

The results of the calculations for the structure shown in Fig. 2 with different values of periodicity are shown in Fig. 5 for the case of $d = 50\mu m$. The total thermal conductance for the small periods is monotonically increasing with increasing filling fraction. This comes from the fact that gratings with higher filling fractions feature more SiC material that is located near the adjacent SiC slab. This then naturally facilitates higher evanescent coupling. However, for the case of $d = 50\mu m$ with the periodicity of $P = 10\mu m$, a peak in thermal transfer is achieved for a value of the filling fraction which is neither 0 nor 1. Noting the fact that the phononic resonance wavelength of the SiC is around $10\mu m$, one can expect Mie resonances of the beams to become important in this case. Such resonances can enhance the thermal transfer and give rise to the highest value of the thermal conductance for a non-unity filling fraction. Note that in this case, the result of effective medium theory has the largest inaccuracy. This is expected since in this case the periodicity is the largest compared with the two other cases ($P = 1\mu m$ and $P = 0.1\mu m$).

The contributions of different frequencies to the thermal conductance for the case of $d = 50\mu m$ are shown in Fig. 6. In this figure, the frequency spectra of the thermal conductance are plotted for three selected filling fractions and for different periodicities. Considering arrays with a periodicity of $P = 10\mu m$, one can see that the thermal conductance for the periodic structure with a filling fraction of $FF = 0.7$ is higher compared with the planar structure. From this figure, it can be seen that this is due to resonant channels which contribute to the thermal conductance, significantly.

For the case of $d = 50\mu m$, thermal conductance is also calculated based on the far-field approximation (FFA). As we expect, this approximation gives a lower value than the exact calculation because it neglects contributions to the thermal transfer arising from multiple reflections of the thermal radiation. However, it is still consistent with the fact that the thermal transfer achieves its maximum for a non-unity filling fraction in the case of $P = 10\mu m$.

By decreasing the distance from $d = 50\mu m$ to $d = 5\mu m$, the thermal conductance for different filling fractions and periodicities increases but still becomes maximum for a non-planar structure at $P = 10\mu m$ (See

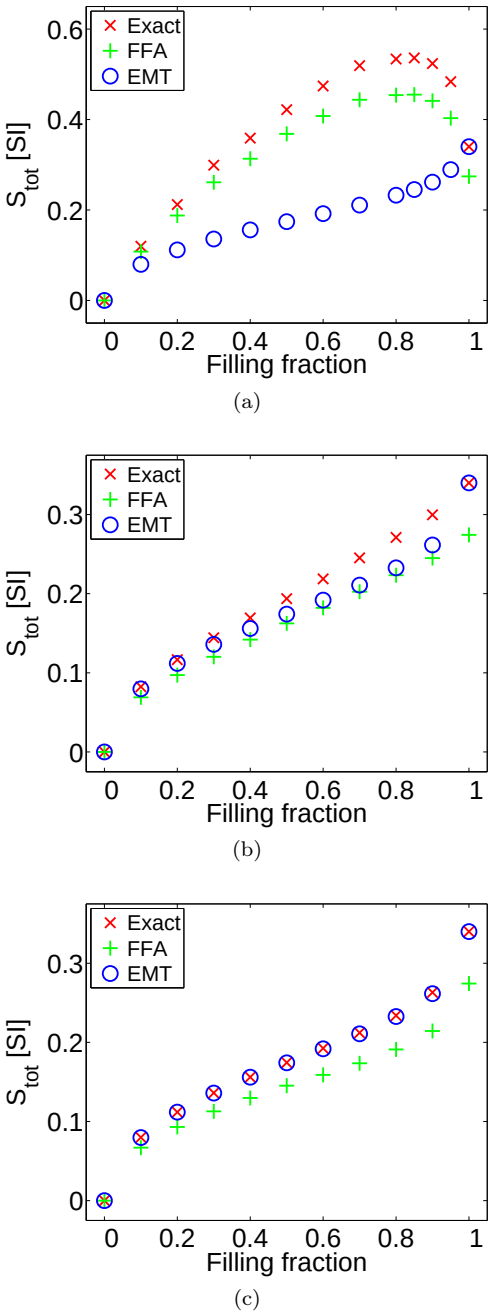

Figure 5: Total thermal conductance for the structure shown in Fig. 2 with $d = 50\mu m$ and different values of filling fraction with the periodicity of (a) $P = 10\mu m$ (b) $P = 1\mu m$ (c) $P = 0.1\mu m$.

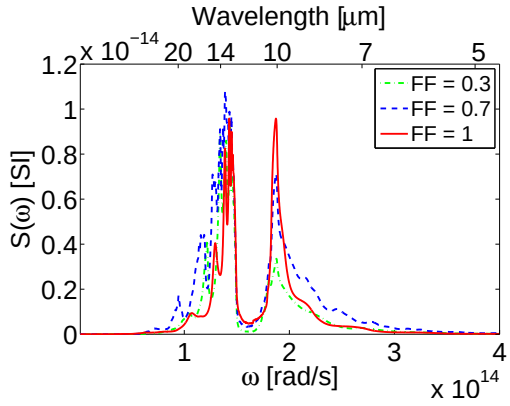

(a)

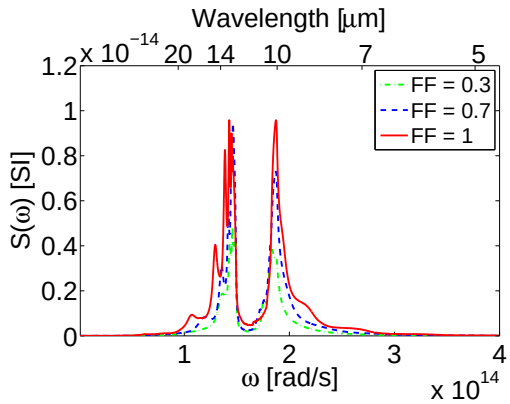

(b)

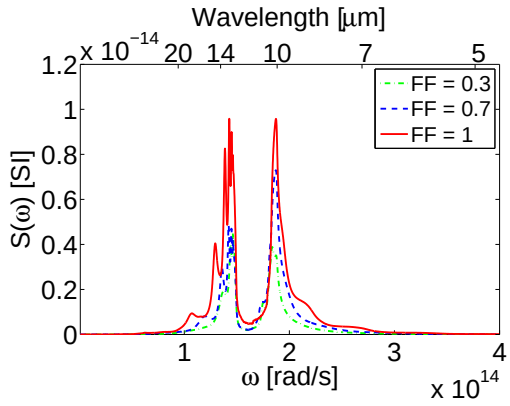

(c)

Figure 6: Thermal conductance frequency spectrum for the structure shown in Fig. 2 with $d = 50\mu m$ and different values of filling fraction with the periodicity of (a) $P = 10\mu m$ (b) $P = 1\mu m$ (c) $P = 0.1\mu m$.

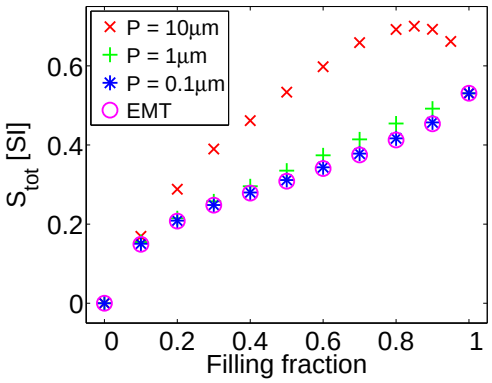

(a)

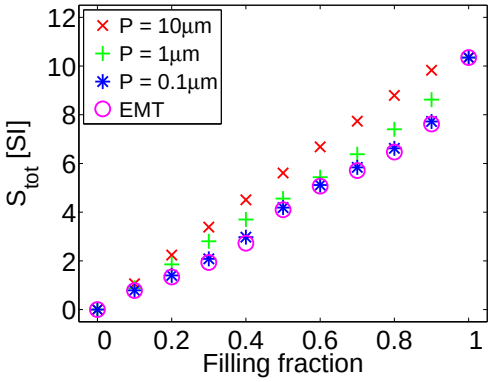

(b)

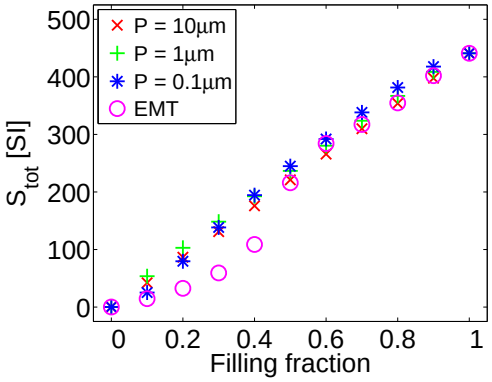

(c)

Figure 7: Total thermal conductance for the structure shown in Fig. 2 with different values of filling fraction and periodicity for (a) $d = 5\mu m$ (b) $d = 0.5\mu m$ (c) $d = 0.05\mu m$.

Fig. 7a). This shows a transition regime, in which both the near-field effect and Mie-resonances are helping to achieve a higher thermal conductance.

However, as Figs. 7b and 7c show, by further decreasing the distance, we reach a regime in which the thermal conductance monotonically increases with increasing filling fraction. Note that this increase is not necessarily linear with the filling fraction. However this increase becomes more linear for large values of the periodicity. This again is consistent with our intuition that for large values of periodicity, the interference between neighboring beams is negligible and that the modified proximity approximation becomes more accurate.

By decreasing the distance, the spectral contributions to the thermal conductance also change. As the distance

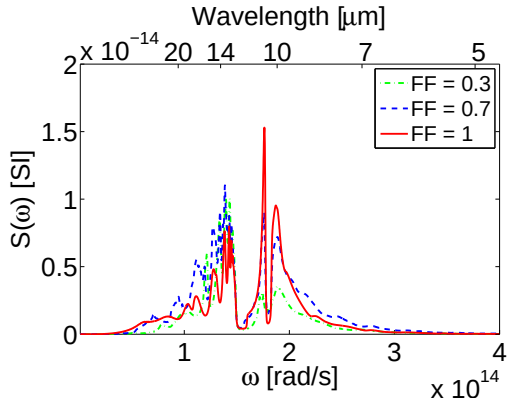

(a)

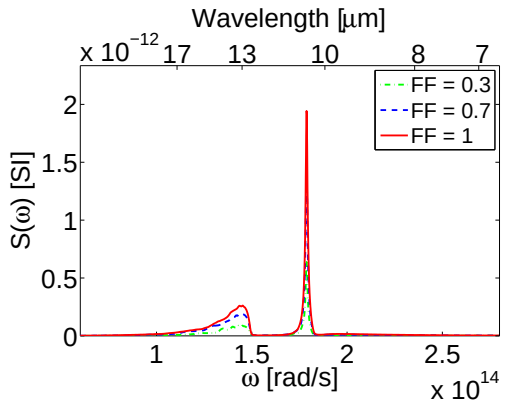

(b)

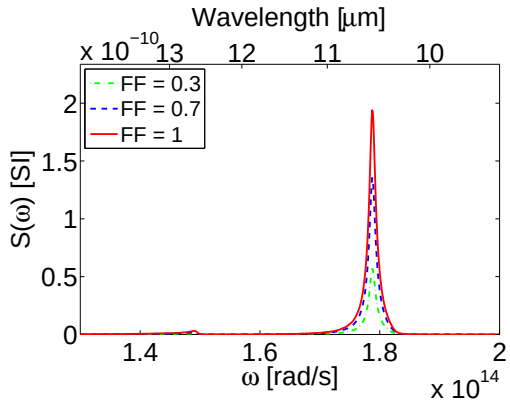

(c)

Figure 8: Thermal conductance frequency spectrum for the structure shown in Fig. 2 with the periodicity of $P = 10\mu m$ and different values of filling fraction for (a) $d = 5\mu m$ (b) $d = 0.5\mu m$ (c) $d = 0.05\mu m$.

decreases, the frequency spectrum of the thermal conductance becomes more concentrated around the surface phonon polariton resonance frequency of a SiC/Air interface. This can be seen from Fig. 8, which shows the frequency spectrum of the thermal conductance for distances of $d = 5\mu m$, $d = 0.5\mu m$, and $d = 0.05\mu m$ in the case of periodicity of $P = 10\mu m$.

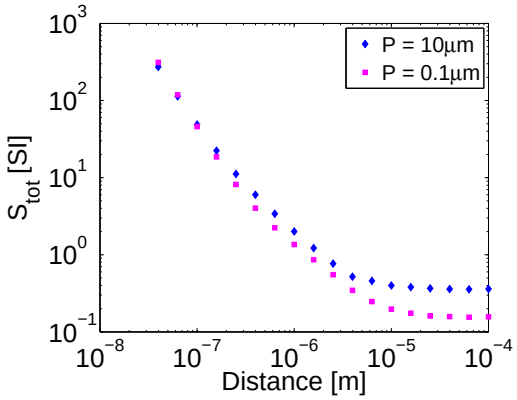

Figure 9: Variation of the total thermal conductance as a function of distance for the structure shown in Fig. 2 with $FF = 0.4$ and $d_{beam} = 5\mu m$. Calculations are done for two periodicities $P = 0.1\mu m$ and $P = 10\mu m$.

Finally, the variation of the thermal conductance with distance for two arrays of beams with periodicities of $P = 10\mu m$ and $P = 0.1\mu m$ (with $d_{beam} = 5\mu m$ and filling fraction of 0.4) is shown in Fig. 9. As it can be seen from the figure, for large distances, the thermal conductance is higher for the array with larger periodicity ($P = 10\mu m$). This can again be attributed to the Mie resonances of the periodic structure with larger periodicity. However, for the very small distances, $d < 0.05\mu m$, the structure with smaller periodicity will have even higher thermal conductance. Note that the thermal conductance in this near-field regime is mainly concentrated around the SiC surface phonon polariton frequency. Moreover, the curve shows that the dependence in this regime is nearly as d^{-2}; however it shows small deviations for the two different periodicities.

One important feature of our method is that it can be used in this way for calculation of thermal transfer between a slab and a particle of any size or shape. This comes from the fact that for sufficiently large periodicities, the interference between neighboring particles becomes negligible and the thermal conductance is coming from the sum of the contributions of individual beams. This can be proposed as an alternative method for calculation of thermal conductance between e.g. a sphere and a slab that has been done in several methods in several references[15–17].

CONCLUSIONS:

In this paper, we have developed a formalism for calculating the thermal transfer in periodic structures with building blocks of arbitrary size and shape. We applied this method to obtain the thermal conductance between a slab of SiC and an array of SiC beams of rectangular cross section. The obtained results show that, thermal conductance in these cases can accurately be obtained through

incorporation of some of the first harmonics. Moreover, results show that the thermal transfer changes monotonically with increasing filling fraction for the cases that distances are much smaller than the SPhP resonance wavelength. However, this trend breaks down for the case that distances are on the same order of magnitude as the pertinent resonance wavelength. Results show that arrays with larger periodicity but with the same filling fraction show increased thermal transfer in the far-field regime. However, the reverse holds in the near-field regime.

Our method, in the case of incorporating just one harmonic reproduces the results obtained by the effective medium theory. In this regard, this method can be used to determine the accuracy of the effective medium theory for specific structures of interest. According to the numerical results obtained, as we expect, by decreasing the periodicity of the structure to the subwavelength regime compared with the relevant resonance wavelengths in the system, effective medium theory becomes increasingly accurate.

This method can also be used to analyze the thermal transfer between structures in which one of the materials is composed of an array of beams. Since in the limit of large periodicity, the interference effects between particles become negligible, this method poses itself to be used for calculation of thermal transfer between a slab and arbitrarily shaped particles. For the reasons above, we believe that the presented technique will prove versatile for calculating and optimizing the thermal transfer between wide varieties of practical structures.

* chalabi@stanford.edu
† mehasman@technion.ac.il
‡ brongersma@stanford.edu

[1] S. Basu, Y.-B. Chen, and Z. M. Zhang, International Journal of Energy Research **31**, 689 (2007).
[2] S. Y. Lin, J. Moreno, and J. G. Fleming, Applied Physics Letters **83**, 380 (2003).
[3] Y. De Wilde, F. Formanek, R. Carminati, B. Gralak, P.-A. Lemoine, K. Joulain, J.-P. Mulet, Y. Chen, and J.-J. Greffet, Nature **444**, 740 (2006).
[4] J. A. Schuller, T. Taubner, and M. L. Brongersma, Nature Photonics **3**, 658 (2009).
[5] N. Dahan, A. Niv, G. Biener, Y. Gorodetski, V. Kleiner, and E. Hasman, Physical Review B **76**, 45427 (2007).
[6] N. Shitrit, I. Yulevich, E. Maguid, D. Ozeri, D. Veksler, V. Kleiner, and E. Hasman, Science (New York, N.Y.) **340**, 724 (2013).
[7] N. Dahan, Y. Gorodetski, K. Frischwasser, V. Kleiner, and E. Hasman, Physical review letters **105**, 136402 (2010).
[8] M. Planck, Blakiston's Son & Co (1914).
[9] D. Polder and M. Van Hove, Physical Review B **4**, 3303 (1971).
[10] A. Shchegrov, K. Joulain, R. Carminati, and J.-J. Greffet, Physical Review Letters **85**, 1548 (2000).
[11] J.-P. Mulet, K. Joulain, R. Carminati, and J.-J. Greffet, Microscale Thermophysical Engineering **6**, 209 (2002).
[12] M. Krüger, G. Bimonte, T. Emig, and M. Kardar, Physical Review B **86**, 115423 (2012), arXiv:1207.0374.
[13] M. Francoeur, M. P. Mengüç, and R. Vaillon, Journal of Physics D: Applied Physics **43**, 075501 (2010).
[14] M. Francoeur, M. P. Mengüç, and R. Vaillon, Physical Review B **84**, 075436 (2011).
[15] M. Krüger, T. Emig, and M. Kardar, Physical Review Letters **106**, 210404 (2011).
[16] C. Otey and S. Fan, Physical Review B **84**, 245431 (2011), arXiv:1103.2668.
[17] A. P. McCauley, M. T. H. Reid, M. Krüger, and S. G. Johnson, Physical Review B **85**, 165104 (2012).
[18] M. T. H. Reid, A. W. Rodriguez, and S. G. Johnson, Proceedings of the IEEE **101**, 531 (2013), arXiv:1207.4222.
[19] S.-A. Biehs, F. S. S. Rosa, and P. Ben-Abdallah, Applied Physics Letters **98**, 243102 (2011), arXiv:1105.3745.
[20] S. Basu and L. Wang, Applied Physics Letters **102**, 53101 (2013).
[21] S.-A. Biehs, M. Tschikin, and P. Ben-Abdallah, Physical Review Letters **109**, 104301 (2012).
[22] S.-A. Biehs, M. Tschikin, R. Messina, and P. Ben-Abdallah, Applied Physics Letters **102**, 131106 (2013), arXiv:1302.3782.
[23] S.-A. Biehs, P. Ben-Abdallah, F. S. S. Rosa, K. Joulain, and J.-J. Greffet, Optics express **19 Suppl 5**, A1088 (2011).
[24] L. Wang, A. Haider, and Z. Zhang, Journal of Quantitative Spectroscopy and Radiative Transfer **132**, 52 (2014).
[25] S. Han, Physical Review B **80**, 155108 (2009).
[26] R. Guérout, J. Lussange, F. S. S. Rosa, J. P. Hugonin, D. A. R. Dalvit, J. J. Greffet, A. Lambrecht, and S. Reynaud, Physical Review B **85**, 180301 (2012), arXiv:1203.1496.
[27] J. Lussange, R. Guérout, F. S. S. Rosa, J.-J. Greffet, A. Lambrecht, and S. Reynaud, Physical Review B **86**, 085432 (2012), arXiv:1206.0211.
[28] R. Messina and M. Antezza, Physical Review A **89**, 052104 (2014).
[29] A. W. Rodriguez, O. Ilic, P. Bermel, I. Celanovic, J. D. Joannopoulos, M. Soljačić, and S. G. Johnson, Physical Review Letters **107**, 114302 (2011).
[30] K. Sasihithlu and A. Narayanaswamy, Physical Review B **83**, 161406 (2011).
[31] E. Rousseau, A. Siria, G. Jourdan, S. Volz, F. Comin, J. Chevrier, and J.-J. Greffet, Nature Photonics **3**, 514 (2009).
[32] C. R. Otey, L. Zhu, S. Sandhu, and S. Fan, Journal of Quantitative Spectroscopy and Radiative Transfer **132**, 3 (2014).
[33] G. Bimonte, Physical Review A **80**, 042102 (2009).
[34] A. W. Rodriguez, M. T. H. Reid, and S. G. Johnson, Physical Review B **86**, 220302 (2012).
[35] B. Liu and S. Shen, Physical Review B **87**, 115403 (2013).
[36] M. G. Moharam, E. B. Grann, D. A. Pommet, and T. K. Gaylord, Journal of the Optical Society of America A **12**, 1068 (1995).
[37] M. G. Moharam, D. A. Pommet, E. B. Grann, and T. K. Gaylord, Journal of the Optical Society of America A **12**, 1077 (1995).
[38] J. E. Sipe, Journal of the Optical Society of America B **4**,

481 (1987).
[39] See Supplemental Material at [URL will be inserted by publisher] for methods and theoretical derivations.
[40] W. Eckhardt, Optics Communications **41**, 305 (1982).
[41] K. Joulain, J.-P. Mulet, F. Marquier, R. Carminati, and J.-J. Greffet, Surface Science Reports **57**, 59 (2005), arXiv:0504068 [physics].
[42] D. L. Jordan, G. D. Lewis, and E. Jakeman, Applied optics **35**, 3583 (1996).
[43] W. Spitzer, D. Kleinman, and D. Walsh, Physical Review **113**, 127 (1959).
[44] W. Spitzer, D. Kleinman, and C. Frosch, Physical Review **113**, 133 (1959).
[45] G. Peter Lepage, Journal of Computational Physics **27**, 192 (1978).
[46] W. Gropp, E. Lusk, and A. Skjellum, Computers & Mathematics with Applications **40**, 419 (2000).
[47] B. Bai and L. Li, Journal of Optics A: Pure and Applied Optics **7**, 783 (2005).